J Mater Sci (2016) 51:5259–5270

In vitro biocompatibility of anodized titanium with deposited silver nanodendrites

Mariusz Kaczmarek[1,*], Karolina Jurczyk[2], Jeremiasz K. Koper[3], Anna Paszel-Jaworska[4], Aleksandra Romaniuk[4], Natalia Lipińska[4], Jakub Żurawski[5], Paulina Urbaniak[6], Jarosław Jakubowicz[3], and Mieczysława U. Jurczyk[7]

[1] *Department of Immunology, Chair of Clinical Immunology, Poznan University of Medical Sciences, Rokietnicka 5D, 60-806 Poznan, Poland*
[2] *Department of Conservative Dentistry and Periodontology, Poznan University of Medical Sciences, Bukowska 70, 60-812 Poznan, Poland*
[3] *Institute of Materials Science and Engineering, Poznan University of Technology, Jana Pawla II 24, 61-138 Poznan, Poland*
[4] *Department of Clinical Chemistry and Molecular Diagnostics, Poznan University of Medical Sciences, Przybyszewskiego 49, 60-355 Poznan, Poland*
[5] *Department of Immunobiochemistry, Chair of Biology and Environmental Sciences, Poznan University of Medical Sciences, Rokietnicka 8, 60-806 Poznan, Poland*
[6] *Department of Cell Biology, Poznan University of Medical Sciences, Rokietnicka 5D, 60-806 Poznan, Poland*
[7] *Division Mother's and Child's Health, Poznan University of Medical Sciences, Polna 33, 60-535 Poznan, Poland*

Received: 14 December 2015
Accepted: 9 February 2016
Published online: 23 February 2016

ABSTRACT

Engineers searching new dental biomaterials try to modify the structure of the material in order to achieve the best performance as well as increased migration and proliferation of cells involved in the osseointegration of the implant. In this work we show in vitro test results of the Ti, which was anodically oxidized at high voltages with additionally deposited silver in the form of nanodendrites. The in vitro cytocompatibility of these materials was evaluated and compared with a conventional microcrystalline titanium. During the studies, established cell line of human gingival fibroblasts (HGF) and osteoblasts were cultured in the presence of tested materials, and its survival rate and proliferation activity were examined. Titanium samples modified with silver has a higher degree of biocompatibility in comparison with the unmodified reference material. Cells in contact with studied material showed a higher relative viability potential, stable level of proliferation activity, and lower rate of mortality. Biocompatibility tests carried out indicate that the anodically oxidized titanium at high voltages with additionally deposited nanosilver could be a possible candidate for dental implants and other medicinal applications.

Address correspondence to E-mail: markacz@ump.edu.pl

DOI 10.1007/s10853-016-9829-3

Introduction

Titanium (Ti) and its alloys are most useful and most often investigated metallic biomaterials. Titanium possesses high strength to density ratio, relatively low Young modulus value, very good corrosion resistance, and biocompatibility. For providing fast osseointegration and long-term usage in the human body, the implant surface should be modified, i.e., it should be rough or porous, oxidized, and covered by biocompatible coating including calcium–phosphate compounds [1–3]. Surfaces showing, micro-, and nanoirregularities are useful in biocompatibility improvements [4].

Among many surface treatment technologies applied for Ti, the electrochemical one is very useful, giving surface roughening and new chemical and phase composition, which improve surface biocompatibility [5–7]. Anodic oxidation results in the formation of rough titanium oxide, which improves osseointegration. The oxidation process can be done in standard conditions as well as can be supported by spark-discharge process in the plasma electrolytic oxidation (PEO), done at high voltages [8–10]. As the results, formation of different size pores or cavities as well as nanotubes are possible [11–13]. The anodically oxidized titanium-based dental implants are commonly available [14]. By carefully choosing the oxidation conditions it is possible to control the oxide thickness, which is correlated with its color [15].

During and after implantation, there is a risk of bacterial attack in the wound tissue. To avoid this inconvenient postoperative effect, an introduction of antibacterial agent into implant surface layer is highly recommended and possible. The commonly known antibacterial agents are silver ions, however it should be noticed, that high silver ion concentration could prevent osseointegration. Cytotoxicity of silver (Ag) nanoparticles at a concentration of 8 $\mu g/cm^2$ to *E. coli* was reported previously [16]. The large surface area to volume ratio of Ag nanoparticles provides good antibacterial behavior [17].

The surface, which is oxidized and has porous topography, is an excellent template for controlled introduction of silver ions. Previously [18] we show preferential deposition mechanism of Ag nanodendrites, which are deposited inside the pits in the oxide layer. Thus we suggest that the surface pits positively effect on both, osteoblast cells and antibacterial nanoparticle attachment.

The aim of this study was to determine of biocompatibility in vitro of the Ti, which was anodically oxidized at high voltages with additionally deposited Ag in the form of nanodendrites. Biocompatibility of the tested material was referred in relation to human osteoblasts and gingival fibroblasts. They are the major cellular elements that determine the osseointegration and the acceptance of implant in the oral cavity.

Materials and methods

Sample preparation

The commercially pure titanium (CP-Ti) with purity >99.6 % (Goodfellow) was used for electrochemical treatment and biocompatibility test. The original ϕ 10 mm Ti rod was cut into a form of small tablets (10 mm diameter and 5 mm height), grinded up to a 1000 sand paper and then polished in Al_2O_3 suspension to a mirror-like surface. The samples were anodically oxidized in home-made Teflon electrochemical cell. The platinum (Pt) electrode was applied as reference electrode. The oxidation process proceeded under Atlas Sollich high voltage potentiostat (300 V/3 A) control. The structural and morphological changes with using broad anodic oxidation voltages were studied in our previous works [19, 20]. In this work for biocompatibility test, samples optimally oxidized at 210 V versus OCP (open circuit potential), at constant time of 30 min were chosen. As the electrolyte, solution of 2 M H_3PO_4 with addition of 1 wt% HF was used. After the oxidation process, the surfaces were rinsed in water and dried under a stream of nitrogen. For obtaining antibacterial characteristics, the surface was electrochemically modified by deposition of Ag nanocrystals, in the form of nanodendrites (nano-trees) using the electrolytic deposition process [18]. The aqueous solution of 0.01 M $AgNO_3$ + 0.01 M HNO_3 composition was served as a substrate for the Ag ions. The Ti samples were immersed in the electrolyte and additionally an Ag plate (8 cm^2) was used to support the transport of the Ag ions and Ag refilling into the electrolyte. An SCE electrode was used as the reference electrode. EG&G electrochemical cell was applied and the electrolyte inside was mixed using magnetic stirring (250 rpm). The process was controlled by a Solartron 1285 potentiostat. The Ag

nanodendrites depositing parameters were as follows: potential −1 V versus OCP, time 60 s, temperature 20 °C. After deposition, the samples were rinsed in distilled water and dried in a stream of nitrogen. For the purpose of this study, materials CP-Ti, anodically oxidized Ti, anodically oxidized with deposited nano-Ag are named as A0, C1, and C2, respectively.

Materials characterization

Structure was determined using Panalytical Empyrean XRD with CuKα_1 radiation, equipped with crystallographic database. Surface topography was determined using Tescan SEM model Vega 5135 equipped with PGT model Prism 200 Avalon EDS, Leica DCM 3D confocal microscope with EPI 20X-L objective, Quesant Q-scope 250 AFM. The AFM tapping mode was applied during surface scanning. The Nanoandmore probes (with pre-mounted Nanosensors SupersharpSilicon^{TM}) were used in the surface scanning.

In vitro biocompatibility studies

Cell cultures

Established line of human gingival fibroblasts HGF-1 (ATCC® CRL-2014^{TM}) and human osteoblast U-2 OS (ATCC®HTB-96^{TM}) were used for the study. Cell lines were derived from ATCC collection. HGF-1 cells were cultured in DMEM/Ham's F12 media (mixed in 1:1) with L-glutamine and 15 mM HEPES, supplemented with 10 % fetal bovine serum (FBS) and 1 % antibiotic solution (10,000 U penicillin, 10 mg/ml streptomycin, 25 mg/ml amphotericin B). U-2 OS cells were cultured in DMEM medium only supplemented as described above. Cells were cultured under standard conditions, in plastic plates in an incubator at 37 °C temperature, in atmosphere of 5 % CO_2 and increased humidity level of 95 %. When the cells reached confluent monolayers (~90 % of cells), the culture media were removed and cells were washed with phosphate-buffered saline (PBS). After removing PBS, the cells were harvested from the surface of plates using a 0.25 % Trypsin–EDTA. The cells were counted using a Fuchs-Rosenthal's hematologic camera. Thus prepared cells were placed on the surface of the tested samples.

In vitro evaluation

Before testing, the samples of the material were sterilized using an autoclave at 120 °C for 15 min. Sterile samples were placed in 24-well culture plates, pre-filled with 1 ml of culture medium. Approximately 3×10^4 of cells were placed directly on the surface of studied material samples. Cultures were grown for 72 and 96 h. To ensure sterile conditions during the analyses, a chamber with laminar air flow and disposable sterile equipment were used.

Imaging of samples using fluorescence microscopy

HGF-1 fibroblasts and U-2 OS osteoblasts growing on the tested materials were imaged with a fluorescent microscope after 96 h. Cells were stained with a thiazole orange (TO). This fluorescent dye penetrates the cell membrane of living cells and bind RNA. Microscopic images of cells growing on the tested samples were archived within 10 min with a fluorescence microscope using appropriate color filters, at a magnification of 40, 100, 400, and 1000 fold.

Cell viability assay (MTT cytotoxicity test)

To evaluate the cytotoxicity of the tested materials the MTT assay was performed. Cytotoxicity level was assessed by determining the percentage of dead cells as well as the degree of inhibition of their growth. During the test, the water-soluble MTT tetrazolium salts (3-(4,5-dimethylthiazol-2-yl)-2,5-diphenyltetrazolium bromide) are reduced to a blue–purple insoluble formazan crystals. The reduction reaction occurs in the presence of the active mitochondrial dehydrogenase, only in living cells. Finally, the formazan crystals are extracted from the cells with a solubilizing solution (10 % SDS in 0.01 M HCl). The intensity of the color reaction is directly proportional to the number of living cells. During analyses cells were cultured directly on material samples located in the complete culture media supplemented as described above in 24-well culture plate. After 72 and 96 h of culture on the surface of the tested samples 100 µl of fresh culture media and 10 µl of a solution of MTT (5 mg/ml thiazolyl blue Tetrazolium Bromide) were applied. Samples were then incubated for 4 h under standard conditions. Finally, the formazan crystals were released from the cells by adding 100 µl of a solubilizing solution. After overnight incubation, the

absorbance of solutions using a microtiter reader (Multiscan, Labsystems) at two wavelengths: $\lambda = 570$ and 690 nm. The viability of cells growing on the tested material was expressed in relation to the viability of cells growing directly on culture plate surface without any material (control samples) as well as growing simultaneously on a sample of the reference material (A0 samples). Results were presented as a Relative Viability of Cells value (RVC), which was calculated from the formula:

$$\mathrm{RVC}\ [\%] = \left[\frac{(a-b)}{(c-b)}\right] \times 100$$

a absorbance of the tested sample; *b* absorbance of the blank control (reaction without the cells); *c* absorbance of the control grown on the reference material.

Evaluation of a cell cycle

After 72 and 96 h of culture, cells covering the material samples were transferred to new plastic tubes. Next, the cells were detached from the surface of the samples with trypsin. Harvested cells were resuspended in a fresh DMEM medium and centrifuged at 1000 rpm for 5 min at room temperature. After discarding, the supernatant cells were washed once with PBS. Finally, to the cell pellets a solution of propidium iodide (PI) and RNase was added, and then incubated for 1 h at 37 °C in the dark. Cells stained with PI were evaluated using the flow cytometer FACSCanto (BD Biosciences). Histograms obtained during the evaluation were analyzed by FACS Diva software. During the analysis, the mean fluorescent intensity (MFI) of stained cells was measured. The percentage of cells in S-phase of the cell cycle corresponds to proliferative activity of the cells grown on the studied material. In addition, on the basis of the cytometric histogram results, the estimated percentage of dead cells as well as cells in the G2/M phase, preceding the process of mitosis, were determined.

Results

Structure properties

Study of Ti surface topography and its properties after different processing conditions of high voltage anodic oxidation was described in previous manuscripts [19, 20]. For the in vitro tests, the surface was oxidized at 210 V for 30 min in 2 M H_3PO_4 + 1 wt% HF electrolyte (Fig. 1), which showed optimum properties, useful for implant applications [19, 20]. The surface treated at these conditions has 3D scaffold morphology with interconnected pores. The surface pores have elongated in plane channel-type form, which were formed by the fusion of the circular pores lying close to each other during anodization. The roughness (Table 1) and morphology of the Ti after anodic oxidation predisposes the surface for implant application. The differences in both Sv and Sz roughness parameters, measured using different techniques (Table 1), are the consequence of different area analysis in AFM and confocal microscopes, however Sa roughness is comparable, independent of the analyzed area.

The electrochemical silver deposition, done on the oxidized Ti at conditions presented in experimental paragraph, resulted in the formation of highly developed nanoparticles in the form of dendrites (Fig. 2). The nanodendrites start to grow from bottom of the surface pores (Fig. 2a, b), formed in the anodic

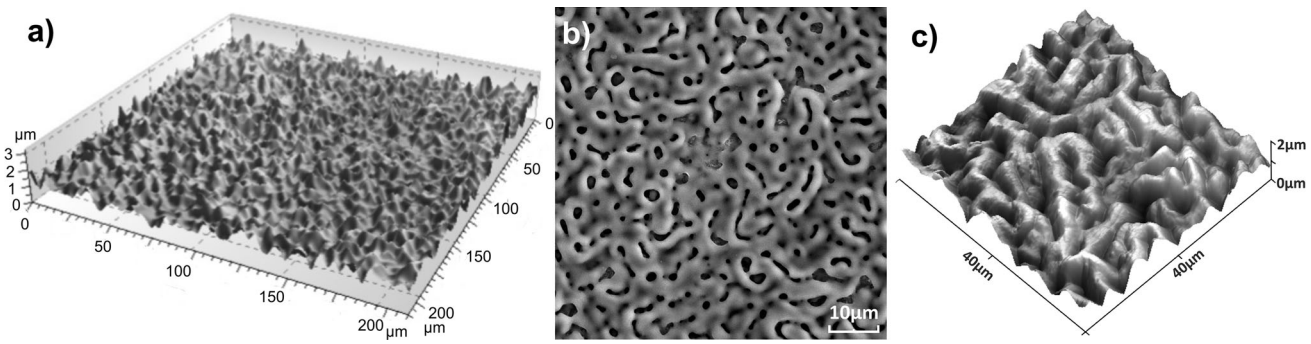

Figure 1 Confocal (**a**), SEM (**b**), and AFM (**c**) pictures of anodically oxidized titanium.

oxidation process. These surface pores support preferential ions flow from the electrolyte, giving formation of nanodendrites. The Ag nanodendrites are composed of mainly rod-type stem, from which branched arms oriented at about 60° propagate (Fig. 2b). The Ag nanodendrites have uniform geometry and a relatively large specific surface area, which should be useful in antibacterial action. The EDS analysis of the deposited Ag nanodendrites (Fig. 2c) showed the presence of Ag on the sample surface. The chemical composition of the nanoparticles was measured in many different points, however the large spot of the X-ray beam, results not only in particle characterization, but Ti substrate detection too. Moreover phosphorus content was also detected as the effect of phosphorus implantation from the electrolyte during anodic oxidation. The phosphorus content can act positively in bone through hydroxyapatite formation. In the EDS spectrum the peaks corresponding to Ag are the main peaks. The Ag nanodendrites have a stem diameter of ~100–150 nm and the length in the range of 5–100 μm, whereas the length of the arms is in the range of 0.2–20 μm. For comparison, Wei et al. [21] use silicon template to produce Ag dendrites of 1–2 μm in stem diameter and 10–50 μm in length. The dendritic silver structures preferentially grow along (111) and (200) directions [21].

Table 1 3D roughness parameters measured on anodically oxidized surface

3D roughness parameter	Method of measurements	
	Confocal	AFM
Sv (μm)	1.452	1.085
Sz (μm)	3.445	1.976
Sa (μm)	0.248	0.240

The XRD spectra shown in Fig. 3 describe Ti surface changes after electrochemical treatment. The Ti after anodic oxidation shows typical α-Ti-type structure (Fig. 3a). No crystalline form of Ti oxides was found, which means that amorphous oxide formation proceeds during applied treatment conditions. The etching of Ti, with the removal of surface oxide is also possible (the electrolyte contains 1 % HF, which strongly acts as oxide etching). The electrochemical silver deposition results are shown in (Fig. 3b, c). The spectrum (b) presents dominant Ti peaks masking the small Ag peaks (relatively very low Ag amount deposited on Ti template) and for comparison the spectrum for deposited silver particles only, after their removal from the surface (c) is shown. The deposited material clearly represents silver (c). As it is seen on the spectrum (b), additional phase TiN was formed during silver deposition process, as the result of Ti and electrolyte ($AgNO_3 + HNO_3$) reaction.

In vitro evaluation results

Fluorescent imaging of samples

Both, HGF-1 fibroblasts and U-2 OS osteoblasts cultured on different types of materials showed different growth patterns, according to the type and composition of the samples as well as their texture. The growth of both cell types on the surface of the control

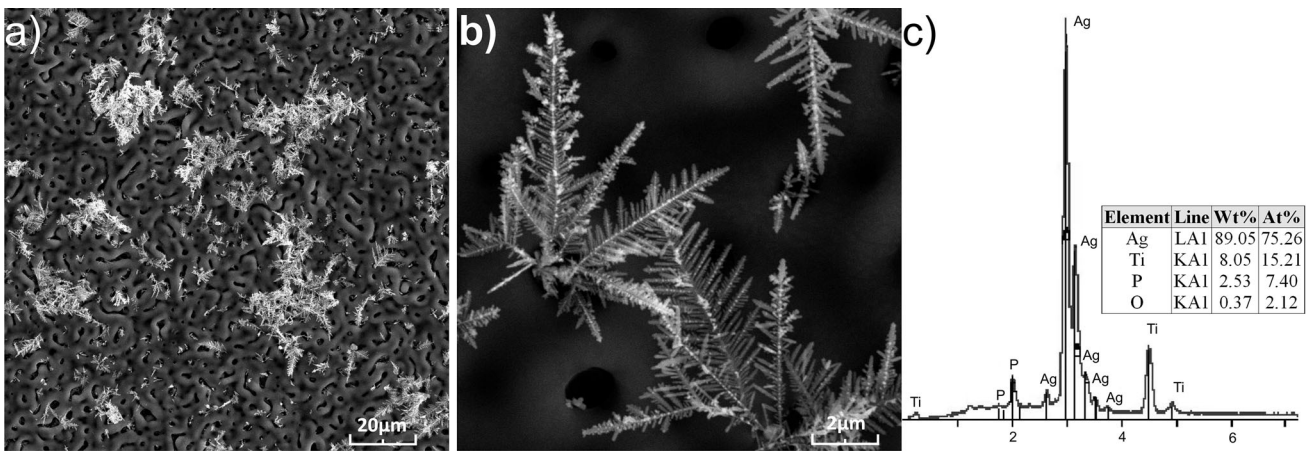

Figure 2 SEM pictures of anodically oxidized titanium with deposited silver nanodendrites (**a**, **b**—different magnifications) and EDS analysis of the silver particles (**c**).

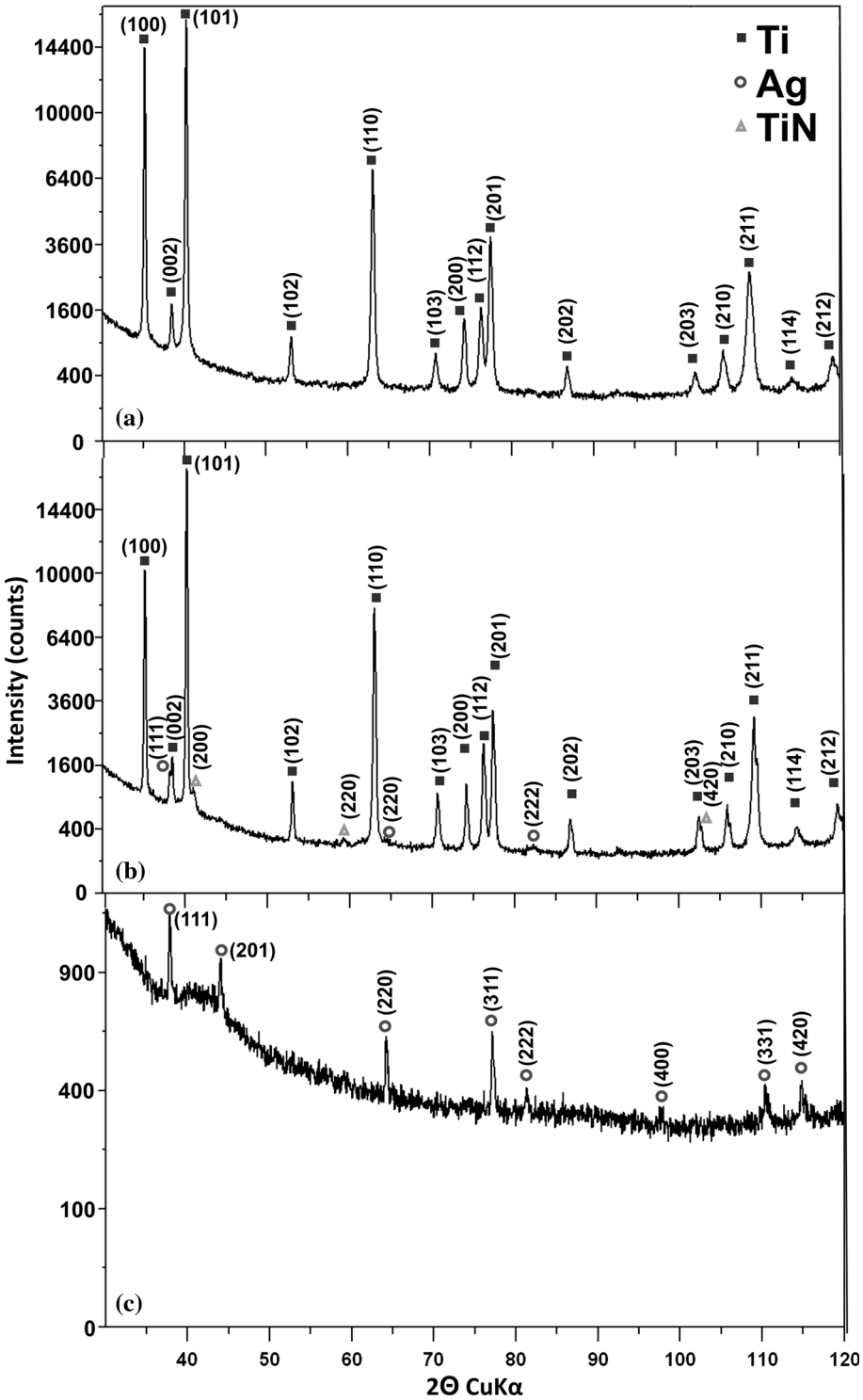

Figure 3 XRD of the titanium after anodic oxidation (**a**), anodic oxidation and silver nanoparticles deposition (**b**), and for comparison only for silver nanoparticles removed from the surface (**c**).

material A0 was homogeneous and showed a parallel and orderly pattern. Particularly fibroblasts were characterized by irregular growth, with the shape of multidirectional network. Their growth on the surface of the anodically oxidized Ti samples with deposited nano-Ag (C2) appeared to be more intense and more regular than on the surface of the anodically oxidized Ti samples without nano-Ag deposits (C1). Osteoblasts also showed much more intensive growth on the surface of C2 sample as compared

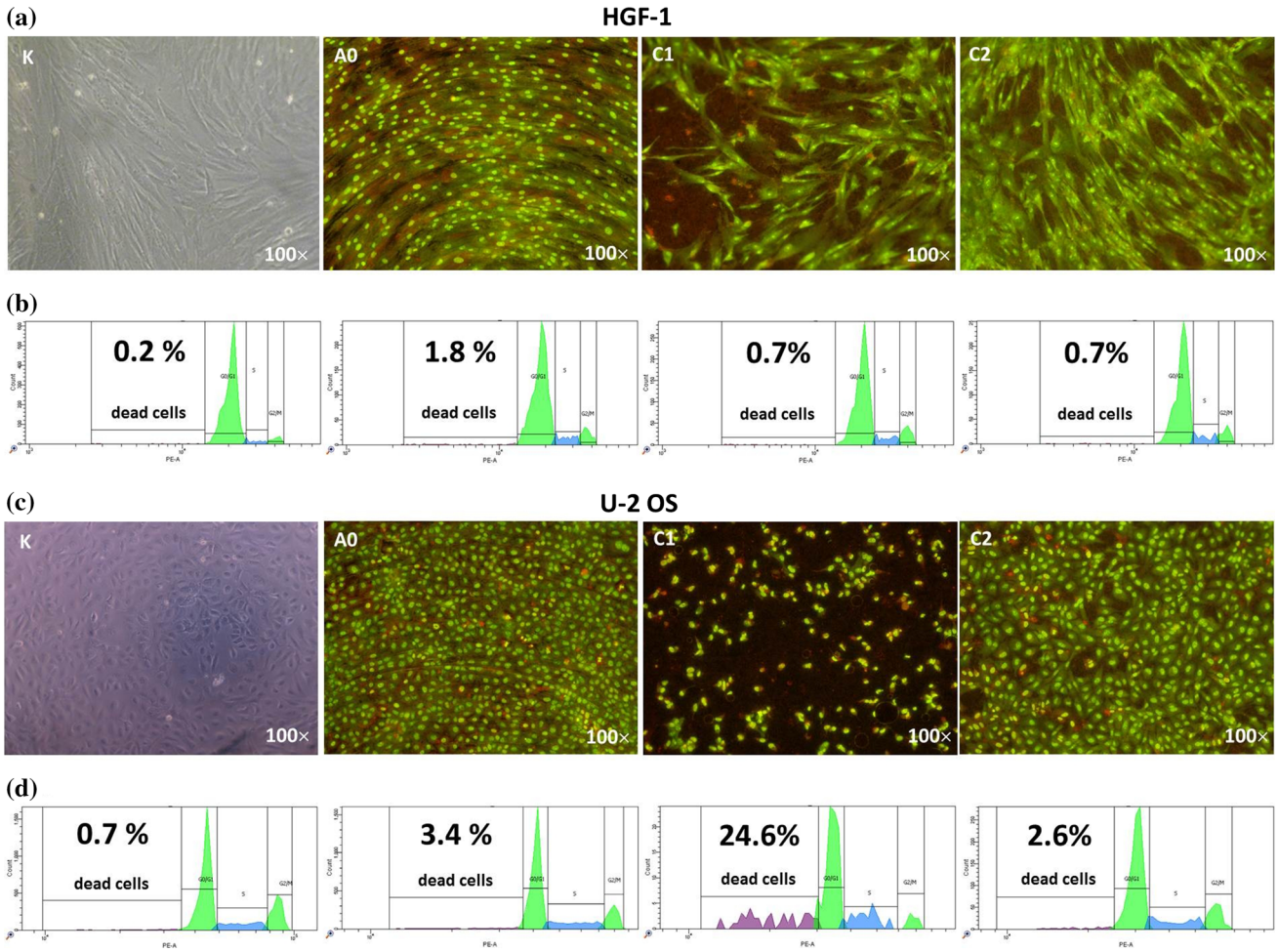

Figure 4 Fluorescent imaging of human gingival fibroblasts (HGF-1) and human osteoblasts (U-2 OS) growing on samples of the tested materials using fluorescent microscopy system (**a**, **c**). Histograms visualizing the phases of the cell cycle, obtained during flow cytometry analysis, with particular indication to the percentage of dead cells (**b**, **d**). Samples: K—cells grown on culture wells without tested materials, A0—CP-Ti, C1—anodically oxidized Ti, C2—anodically oxidized with deposited nano-Ag.

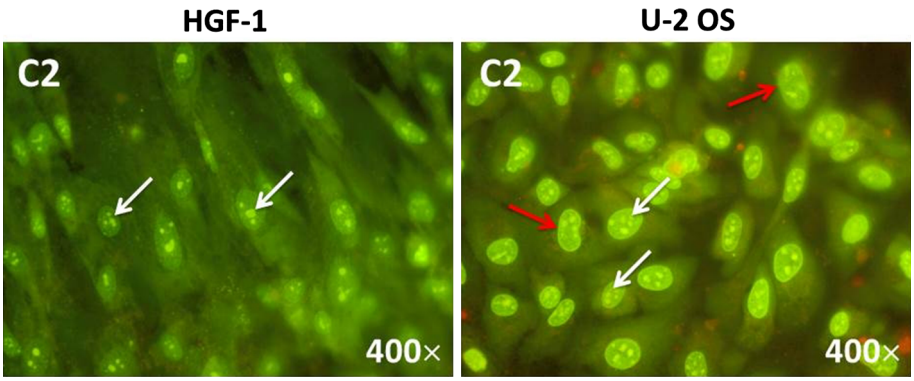

Figure 5 Nucleolus organizer regions within the cell nuclei of HGF-1 fibroblasts and U-2 OS osteoblasts cultured on the surface of the C2 material sample—*white arrows*; cells during division—*red arrows* (TO staining, 400× magnification).

with sample C1. However, their growth on the surface of the C1 material was clearly limited (Fig. 4a, c). Moreover within the cell nuclei numerous nucleolus organizer regions (NOR) were visible (Fig. 5).

Cell viability assay (MTT cytotoxicity test)

First the spontaneous ability to reduce the soluble tetrazolium salt by the tested samples was evaluated

(Fig. 6). During MTT tests two independent cultures for each cell line were made. In each culture, cells were grown in triplicates directly on samples of the test materials. The cultures were performed for 72 and 96 h. As a control of spontaneous growth of cells, the cells were grown directly on culture plates in the wells without the tested material samples (control).

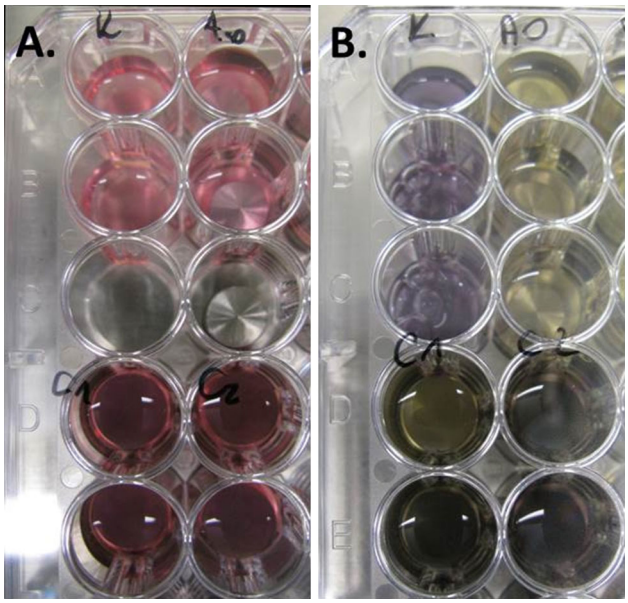

Figure 6 Samples of the A0, C1, and C2 materials placed in the wells with culture media with the addition of MTT solution. Samples before reduction of MTT tetrazolium salt (**a**) and after reduction (**b**).

Simultaneously, cells were cultured on the surface of the reference material (control of cell growth on a reference material, A0). Viability of cells growing on C1 and C2 samples was compared to viability of cells growing in wells without test samples (control) as well as to cells growing on a reference material. MTT tests showed differences in viability potential of HGF-1 and U-2 OS cell lines (Fig. 7). Tested cells showed similar relative viability potential (RVC) in contact with tested samples compared to the control, despite natural diversities between the HGF-1 and U-2 OS lines. Their potential was smaller than potential of control cells. Both cell lines showed higher viable potential in contact with C1 and C2 samples compared to cells growing on A0, however potential of U-2 OS was stronger. Moreover, RVC of both the cell lines increased simultaneously in the course of time.

Evaluation of the cell cycle

The cell cycle of HGF-1 and U-2 OS cells growing on the surface of the tested samples was estimated, using the flow cytometer. The results of the evaluation were visualized in the form of histograms, which allowed to determine the percentage of cells in particular phases of the cell cycle, as well as percentage of dead cells, which died in the course of culture on the surface of tested materials (Fig. 4b, d). HGF-1 fibroblasts cultured on C1 and C2 samples showed decreased proliferative activity in relation to HGF-1 cultured on the

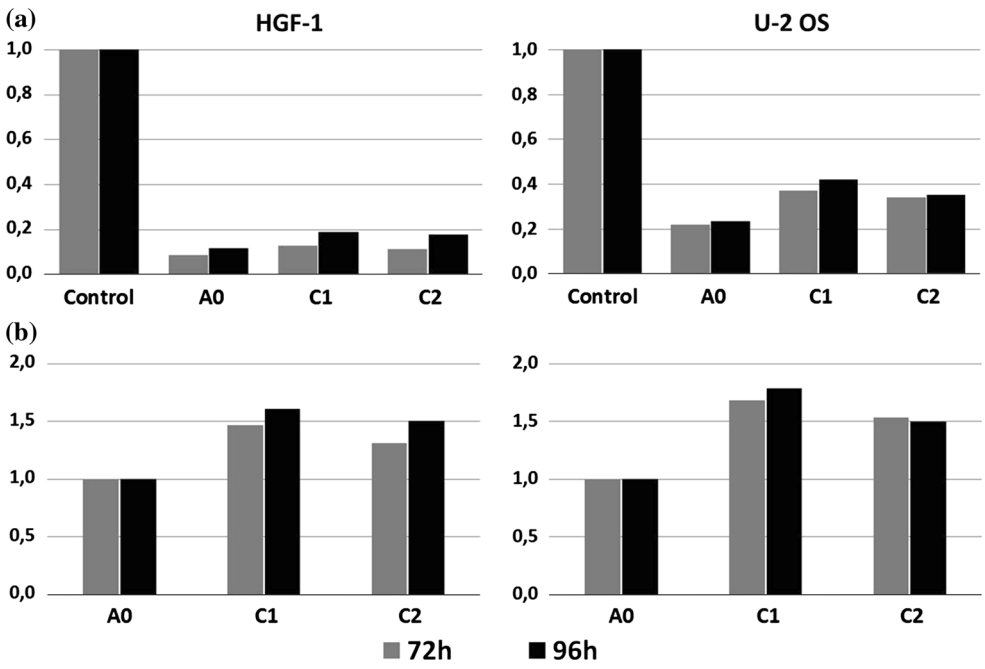

Figure 7 Viability of HGF-1 fibroblasts and U-2 OS osteoblasts cultured on the C1 and C2 samples, relative to cells growing directly on the surface of the culture plates (control) as well as to cells growing on the reference material (A0), in the 72 and 96 h of culture.

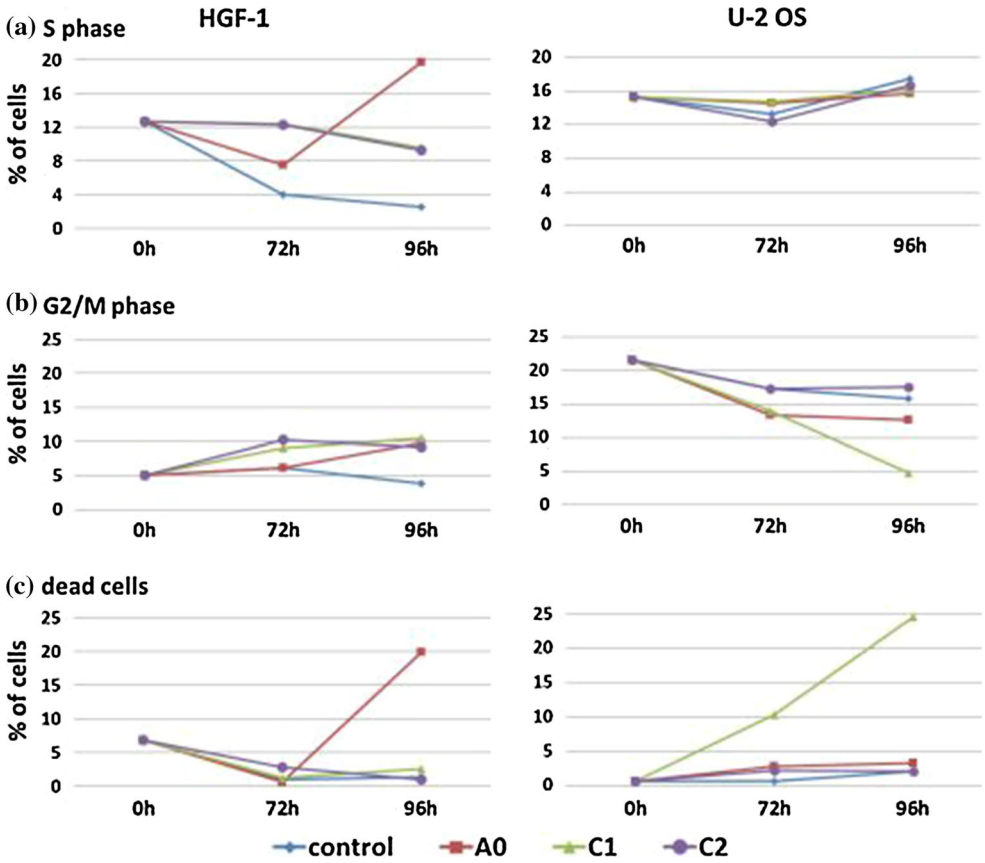

Figure 8 Proportional participation of HGF-1 and U-2 OS cells cultured on the surface of the C1 and C2 material samples in particular phases of the cell cycle. Percentage of cells in the S-phase (proliferative activity; **a**); percentage of cells in the G2/M phase (percentage of cells in the premitotic phase; **b**); percentage of dead cells (apoptotic and/or necrotic cells; **c**).

A0 material. Both cell lines cultured on the C1 and C2 samples compared to those on A0 were characterized by a much lower mortality rate, which was comparable to mortality observed among cells directly growing on a culture plate, without contact with tested materials. U-2 OS cells revealed higher proliferative potential as compared to the HGF-1 cells, independently from time and tested material. Studied osteoblasts cultured on C1 and C2 samples showed lower percentage of cells in the S-phase of the cell cycle as compared to the control, but higher as compared to cells on the surface of the A0 samples. However, during the test the U-2 OS osteoblasts cultured on the C1 samples showed high percentage of dead cells (Fig. 8).

Discussion

The main task is to adjust the structure of the material to achieve increased migration and proliferation of cells involved in the osseointegration of the implant. It is important to create material with high durability and resistance to the environment surrounding the tissue and a low susceptibility to colonization by pathogenic microorganisms. However, till now materials having characteristics identical to natural has not been created. It has been proven that the porous materials in the most accurate way fill these assumptions [5, 9].

The anodic oxidation process done at high voltages is very useful in surface biofunctionalization, i.e., formation of porous, rough, and biocompatible oxide [8–10, 19, 20]. As we have shown in this work, the PEO followed by spark discharge, which proceeds on the Ti surface, results in the formation of highly connected channels in the surface of the oxide layer. The channels support not only bone cell nucleation and growth, but vascularization process too. In this way formation of strong bond between implant material and bone is provided. Thus the process done at high voltages significantly overcomes the conventional low voltage oxidation process [5]. Additionally inside the channel structure, the oxide thickness at pore bottom is lowest, which positively acts on silver ions flow from electrolyte into the surface of highest electrical conductivity (lowest oxide thickness) [18]. The Ag nanodendrites grow inside the pores and forms biocompatible layer with enhanced bacterial

killing properties. Moreover the Ag nanoparticles fixed inside the pores are protected against their removing during implant handling.

The main reason for implantation failure is local inflammation caused by reaction of tissue on the introduction of a foreign body. Cascade of negative events in the organism may be accompanied by the activity of pathogenic microorganisms. Disrupted relationship between host and microflora resulting in disease of the oral structures, mainly include dental caries, gingivitis or periodontitis or peri-implantitis [22]. Peri-implantitis around osseointegrated implants initiated by bacterial infection affect the soft and hard tissues and can lead to bone damage [23]. Some bacteria attached to implanted restorative materials form the biofilm that protects them against antibiotic treatment, leading to antibiotic-resistant periprosthetic infection [24].

Nanostructured biomaterials exhibit exceptional mechanical and surface features [25]. They can mimic the bones, by what are considered the next-generation materials. [26]. The shape, spatial and chemical structure, roughness, and surface energy have impact on the adhesion and proliferation of cells. However, the rough surface of the dental implants can promote the colonization by pathogens [27]. Therefore, the next challenge for the dental implantology is an indication of materials, which will limit the risk of colonization with pathogenic microorganisms. Due to proven antibacterial properties Ag nanoparticles are intensively investigated as a material used in dental applications, mainly as dental fillings or implants [28, 29]. Strong antibacterial features of Ag are associated with the ability of this metal to interact with sulfhydryl groups of proteins as well as with DNA [30]. Ag nanoparticles have activity against Gram-positive and Gram-negative bacteria, fungi, and viruses [31, 32].

However, the use of Ag nanoparticles carries the risk of cytotoxicity causing tissue destruction and local inflammation. Certain Ag compounds exhibited nanotoxicity for HGF [33]. Ag nanoparticles by induction of oxidative stress can be also mutagenic for cells [34]. However, the use of Ag nanoparticles coated on a titanium core seems to be very useful in dental technology. Mei et al. [35] used processes of anodization and Ag plasma immersion ion implantation for production of Ti nanotubes containing Ag nanoparticles. The technology used has confirmed the high biocompatibility of Ti and the antimicrobial effect of the Ag particles, enhanced by the large depth of the deposited Ag. Other group indicated an antibiofilm effect of Ag nanoparticles immobilized on Ti against *Staphylococcus epidermidis*. This activity was related with inhibition of bacteria adhesion and down regulation of transcription of the intercellular adhesion operon (*icaAD*) [36]. Liu et al. proved that Ag nanoparticles promoted proliferation and maturation of preosteoblasts and induced osteogenesis of rat bones, accompanied with suppression of bacterial survival [37].

In our study we examined the biocompatibility of the samples of anodized Ti modified with deposited Ag nanodendrites. Material samples were evaluated based on contact with the HGF and osteoblasts (U-2 OS) cell lines in vitro. Evaluation of fibroblasts and osteoblasts growth served as a model showing the behavior of cells of the soft and hard tissue in contact with the tested material. Cytocompatibility of tested nanosilver–titanium composites was compared to conventional microcrystalline Ti, which served as a reference material. Studies on dental implants are mainly focused on assessing the interaction between materials and bone cells as well as soft tissue, because the process of osseointegration may be disturbed by anomalies and infections of soft tissue [38]. To evaluate the cytocompatibility of the tested samples, in vitro characterization tests in static condition were performed. Samples were tested for cytotoxicity with MTT assay. Proliferative activity of cells directly growing on samples was determined with cytofluorimeter (determination of the percentage of cells in S-phase of the cell cycle stained with PI). Furthermore, cells growing on the tested samples were stained with thiazole orange and visualized in a fluorescence microscope. Our analyses indicated that the nanocrystalline Ti modified with Ag has a higher degree of biocompatibility in comparison with the unmodified reference material, which was microcrystalline Ti. Cells used in the tests showed a higher relative viability potential in contact with tested materials, than cells in contact with the surface of control samples. Both, fibroblasts and osteoblasts showed numerous NOR within the cell nuclei what may serve as an evidence of increased proliferative activity of tested cells. This observation was supported by numerous cells in the process of mitosis. Moreover, cytometric analysis confirmed these results, particularly when tested cells showed the stable level of proliferation activity and lower rate of mortality.

Modification of the titanium through the anodic oxidation process at high voltages with additional deposition of nanosilver can significantly change the properties of the reference material, which can improve its biocompatibility, but also can introduce new quality. The development of such material is a major goal of modern materials science. Anodized titanium modified with deposited silver nanodendrites, the material presented in this report significantly brings us closer to this target.

Acknowledgements

The work has been financed by Polish Ministry of Science and Higher Education within statutory activity.

Compliance with ethical standards

Conflict of interest Authors declare no conflict of interest.

References

[1] Sul YT (2003) The significance of the surface properties of oxidized titanium to the bone response: special emphasis on potential biochemical bonding of oxidized titanium implant. Biomaterials 24:3893–3907

[2] Oh H-J, Lee J-H, Kim Y-J, Suh S-J, Lee J-H, Chi Ch-S (2008) Surface characteristics of porous anodic TiO_2 layer for biomedical applications. Mater Chem Phys 109:10–14

[3] Adamek G, Jakubowicz J (2010) Mechanoelectrochemical synthesis and properties of porous nano-Ti-6Al-4V alloy with hydroxyapatite layer for biomedical applications. Electrochem Commun 12:653–656

[4] Webster TJ, Ejiofor JU (2004) Increased osteoblast adhesion on nanophase metals: Ti, Ti6Al4V, and CoCrMo. Biomaterials 25:4731–4739

[5] Jakubowicz J (2008) Formation of porous TiO_x biomaterias in H_3PO_4 electrolytes. Electrochem Commun 10:735–739

[6] Jakubowicz J, Adamek G, Jurczyk MU, Jurczyk M (2012) 3D surface topography study of the biofunctionalized nanocrystalline Ti-6Zr-4Nb/Ca-P. Mater Charact 70:55–62

[7] Lee J-H, Kim S-E, Kim Y-J, Chi Ch-S, Oh H-J (2006) Effects of microstructure of anodic titania on the formation of bioactive compounds. Mater Chem Phys 98:39–43

[8] Yang B, Uchida M, Kim H-M, Zhang X, Kokubo T (2004) Preparation of bioactive metal via anodic oxidation treatment. Biomaterials 25:1003–1010

[9] Huang P, Xu K-W, Han Y (2005) Preparation and apatite layer formation of plasma electrolytic oxidation film on titanium for biomedical application. Mater Lett 59:185–189

[10] Huang P, Wang F, Xu K, Han Y (2007) Mechanical properties of titania prepared by plasma electrolytic oxidation at different voltages. Surf Coat Technol 201:5168–5171

[11] Yang W-E, Hsu M-L, Lin M-Ch, Chen Z-H, Chen L-K, Huang H-H (2009) Nano/submicron-scale TiO_2 network on titanium surface for dental implant application. J Alloys Compd 479:642–647

[12] Macak JM, Sirotna K, Schmuki P (2005) Self-organized porous titanium oxide prepared in Na_2SO_4/NaF electrolytes. Electrochim Acta 50:3679–3684

[13] Tsuchiya H, Macak JM, Taveira L, Balaur E, Ghicov A, Sirotna K, Shmuki P (2005) Self-organized TiO_2 nanotubes prepared in ammonium fluoride containing acetic acid electrolytes. Electrochem Commun 7:576–580

[14] Le Guehennec L, Soueidan A, Layrolle P, Amouriq Y (2007) Surface treatments of titanium dental implants for rapid osseointegration. Dent Mater 23:844–854

[15] Yang Ch-L, Chen F-L, Chen S-W (2006) Anodization of the dental arch wires. Mater Chem Phys 100:268–274

[16] Rai M, Yadav A, Gade A (2009) Silver nanoparticles as a new generation of antimicrobials. Biotechnol Adv 27:76–83

[17] Chen X, Schleusener HJ (2008) Nanosilver: a nanoproduct in medical application. Toxicol Lett 176:1–12

[18] Jakubowicz J, Koper JK, Adamek G, Połomska M, Wolak J (2015) Silver nano-trees deposited in the pores of anodically oxidized titanium and Ti scaffold. Int J Electrochem Sci 10:4165–4172

[19] Koper JK, Jakubowicz J (2014) Correlation of wettability with surface structure and morphology of the anodically oxidized titanium implants. J Biomater Tissue Eng 4:459–464

[20] Koper JK, Jakubowicz J (2015) Corrosion resistance of porous titanium surface prepared at moderate and high potentials in H_3PO_4/HF electrolytes. Prot Metal Phys Chem Surf 51:295–303

[21] Wei Y, Chen Y, Ye L, Chang P (2011) Preparation of dendritic-like Ag crystals using monocrystalline silicon as template. Mater Res Bull 46:929–936

[22] Allaker RP, Memarzadeh K (2014) Nanoparticles and the control of oral infections. Int J Antimicrob Agents 43:95–104

[23] Mombelli A (2000) Microbiology and antimicrobial therapy of peri-implantitis. Periodontology 2002(28):177–189

[24] Stewart PS, Costerton JW (2001) Antibiotic resistance of bacteria in biofilms. Lancet 358:135–138

[25] Allaker RP, Ren G (2008) Potential impact of nanotechnology on the control of infectious diseases. Trans R Soc Trop Med Hyg 102:1–2

[26] Webster TJ, Ejiofor JU (2004) Increased osteoblast adhesion on nanophase metals: Ti, Ti6Al4V, and CoCrMo. Biomaterials 25:4731–4739

[27] Burgers R, Hahnel S, Reichert TE, Rosentritt M, Behr M, Gerlach T et al (2010) Adhesion of *Candida albicans* to various dental implant surfaces and the influence of salivary pellicle proteins. Acta Biomater 6:2307–2313

[28] Garcia-Contreras R, Argueta-Figueroa L, Mejia-Rubalcava C, Jimenez-Martinez R, Cuevas-Guajardo S, Sanchez-Reyna PA et al (2011) Perspectives for the use of silver nanoparticles in dental practice. Int Dent J 61:297–301

[29] Jurczyk K, Adamek G, Kubicka MM, Jurczyk M (2015) Nanostructured titanium-10 wt% 45S5 bioglass-Ag composite foams for medical applications. Materials 8:1398–1412

[30] Lansdown AB (2006) Silver in health care: antimicrobial effects and safety in use. Curr Probl Dermatol 33:17–34

[31] Sadhasivam S, Shanmugam P, Yun K (2010) Biosynthesis of silver nanoparticles by Streptomyces hygroscopicus and antimicrobial activity against medically important pathogenic microorganisms. Colloids Surf B Biointerfaces. 81:358–362

[32] Lu L, Sun RW, Chen R, Hui CK, Ho CM, Luk JM et al (2008) Silver nanoparticles inhibit hepatitis B virus replication. Antivir Ther. 13:253–262

[33] Park EJ, Yi J, Kim Y, Choi K, Park K (2010) Silver nanoparticles induce cytotoxicity by a Trojan-horse type mechanism. Toxicol In Vitro 24:872–878

[34] Mei N, Zhang Y, Chen Y, Guo X, Ding W, Ali SF et al (2012) Silver nanoparticle-induced mutations and oxidative stress in mouse lymphoma cells. Environ Mol Mutagen 53:409–419

[35] Mei S, Wang H, Wang W, Tong L, Pan H, Ruan C et al (2014) Antibacterial effects and biocompatibility of titanium surfaces with graded silver incorporation in titania nanotubes. Biomaterials 35:4255–4265

[36] Qin H, Cao H, Zhao Y, Zhu C, Cheng T, Wang Q et al (2014) In vitro and in vivo anti-biofilm effects of silver nanoparticles immobilized on titanium. Biomaterials 35:9114–9125

[37] Liu Y, Zheng Z, Zara JN, Hsu C, Soofer DE, Lee KS et al (2012) The antimicrobial and osteoinductive properties of silver nanoparticle/poly (DL-lactic-co-glycolic acid)-coated stainless steel. Biomaterials 33:8745–8756

[38] Hench LL (1991) Bioceramics: from concept to clinic. J Am Ceram Soc 74:1487–1510